



Global scale identification of catchments phosphorus source shifts with urbanization: A phosphate oxygen isotope and Bayesian mixing model approach

Ziteng Wang^a, Fuhong Sun^{a,*}, Qingjun Guo^{b,c}, Daren C. Gooddy^d, Fengchang Wu^{a,*}

^a State Key Laboratory of Environment Criteria and Risk Assessment, Chinese Research Academy of Environmental Sciences, Beijing 100012, China

^b Key Laboratory for Resource Use and Environmental Remediation, Institute of Geographic Sciences and Natural Resources Research, Chinese Academy of Sciences, Beijing 100101, China

^c University of Chinese Academy of Sciences, Beijing 100049, China

^d British Geological Survey, Maclean Building, Wallingford, Oxfordshire OX10 8BB, United Kingdom

ARTICLE INFO

Keywords:

Phosphate oxygen isotopes
P source shifts
Urbanization stage
Driving force
Catchment P management

ABSTRACT

Different scenarios of urban expansion can influence the dynamic characteristics of catchments in terms of phosphorus (P). It is important to identify the changes in P sources that occur during the process of urbanization to develop targeted policies for managing P in catchments. However, there is a knowledge gap in quantifying the variations of potential P sources associated with urbanization. By combining phosphate oxygen isotopes from global catchments with a Bayesian model and the urbanization process, we demonstrate that the characteristics of potential P sources (such as fertilizers, urban wastewater, faeces, and bedrock) change as urban areas expand. Our results indicate that using phosphate oxygen isotopes in conjunction with a Bayesian model provides direct evidence of the proportions of potential P sources. We classify catchment P loadings into three stages based on shifts in potential P sources during urban expansion. During the initial stage of urbanization (urban areas < 1.5 %), urban domestic and industrial wastewater are the main contributors to P loadings in catchments. In the mid-term acceleration stage (1.5 % ≤ urban areas < 3.5 %), efforts to improve wastewater treatment significantly reduce wastewater P input, but the increase in fertilizer P input offsets this reduction in sewage-derived P. In the high-level urbanization stage (urban areas ≥ 3.5 %), the proportions of the four potential P sources tend to stabilize. Remote areas bear the burden of excessive P loadings to meet the growing food demand and improved diets resulting from the increasing urban population. Our findings support the development of strategies for water quality management that better consider the driving forces of urbanization on catchment P loadings.

1. Introduction

The consumption of phosphorus (P) has been rapidly increasing due to the growing human needs to sustain the Green Revolution (Elser and Bennett, 2011; Tilman et al., 2001). Human activities have caused a fourfold increase in P input to the biosphere in recent decades, posing significant pressure on existing phosphate reserves (Bouwman et al., 2013; Powers et al., 2016). This escalating P consumption is beyond the planetary boundaries (Steffen et al., 2015), and has led to the entry of large amounts of anthropogenic P into catchments, primarily driven by the relatively low stoichiometric requirement (Cleveland and Liptzin, 2007). Consequently, this excessive P can enter surrounding water bodies through various pathways, such as pipeline transport and surface

runoff, resulting in eutrophication—a critical global water quality concern (Ho et al., 2019). Therefore, accurate prediction of P inputs to surface water is crucial for effective P management in catchments.

Urban expansion is a highly likely irreversible process that brings about rapid changes in land cover (Gao and O'Neill, 2020), causing substantial concerns about the degradation of Groundwater (Huang et al., 2023; Zhang et al., 2020) and surface aquatic ecosystems (Fu et al., 2021) due to urbanization. As the world's population increasingly urbanizes, the demand for P in food production has intensified (Liang et al., 2020). The process of urbanization has resulted in shifts in the dynamics of P in catchments. With rural labour forces moving to cities, there has been a significant increase in urban populations and a shift towards large-scale farming (Ma et al., 2019; Wang et al., 2021).

* Corresponding authors.

E-mail addresses: sunfhiae@126.com (F. Sun), wufengchang@vip.skleg.cn (F. Wu).

<https://doi.org/10.1016/j.watres.2023.121026>

Received 27 September 2023; Received in revised form 12 December 2023; Accepted 15 December 2023

Available online 16 December 2023

0043-1354/© 2023 Elsevier Ltd. All rights reserved.

Urbanization also influences consumption patterns, with higher per capita income in urban areas compared to rural areas (Bai et al., 2014a). Consequently, there are notable urban–rural differences in food consumption, with urban populations consuming more animal-derived food (Pandey et al., 2020). The proportion of meat consumption continues to increase, necessitating more intensive livestock farming to meet demand. Large quantities of animal excrement are exposed in the surface environment, becoming a significant non-point source of pollution (Bouwman et al., 2013). Accompanied by the process of urbanization, large scale urbanization often results in groundwater contamination worldwide (Bi et al., 2022), they have accelerated the contamination and deterioration of both surface water groundwater quality (Zhang et al., 2019), increase the nutrient salt content of water bodies (Huang et al., 2022). In the process of urban water use, municipal sewage is produced (Larsen et al., 2016). Furthermore, urban water use leads to the production of municipal sewage (Larsen et al., 2016), and the increasing wastewater production and growing treatment facilities associated with urbanization can potentially impact water quality (Tong et al., 2020; Yu et al., 2019). Considering these factors, along with the process of urbanization, different scenarios can drive varying levels of P loadings in catchments. While some studies have explored the impact of urbanization on changes in P content (Huang et al., 2020), P forms (Ryan et al., 2007), and P output (Mao et al., 2023), limited research exists on the multidimensional influences of urbanization that lead to a shift in catchment P sources. Understanding the characteristics of P sources within the urbanization process is vital for effective P management policies.

Amongst the various approaches used for tracing P, the use of phosphate oxygen isotopes ($\delta^{18}\text{O}_{(\text{PO}_4)}$) has gained increasing attention (Goody et al., 2015; Ishida et al., 2019; Tcaci et al., 2019). Although there is only one stable P isotope, the stable isotope ratios of oxygen in PO_4^{3-} can serve as tracers to investigate the P cycle in the environment (Colman, 2002; Liang, 2005; Young et al., 2009). For example, phosphate oxygen isotopes can be used to identify key influencing factors by analysing the differences in $\delta^{18}\text{O}_{(\text{PO}_4)}$ values between rivers and their end-member samples (Davies et al., 2014; Goody et al., 2016; McLaughlin et al., 2006a). Furthermore, the $\delta^{18}\text{O}_{(\text{PO}_4)}$ composition of bottom and suspended sediment can be used to study the effect of internal P release on P loadings in water bodies (Granger et al., 2017; McLaughlin et al., 2006b; Yuan et al., 2022). By determining the $\delta^{18}\text{O}_{(\text{PO}_4)}$ composition of fertilizer, sewage treatment plant outflows, soil and plants, researchers have been able to establish the contributions of P inputs to water body P content (Goody et al., 2018; Ide et al., 2020; Ishida et al., 2019; Wells et al., 2022). Additionally, by measuring $\delta^{18}\text{O}_{(\text{PO}_4)}$ values of rivers and their tributaries, the movement of P in catchments can be demonstrated (Granger et al., 2017; Ji, 2017). Previous studies have contributed to our understandings of P transport in catchments. However, there is limited research to quantifying multiple P sources by the phosphate oxygen isotopes. Liu et al. quantified three potential P sources in the Tuojiang River using a multi-isotope approach and Bayesian model (Liu et al., 2023). We used phosphate oxygen isotopes and multiple models to quantify five external P sources in different reaches of the Yangtze River (Wang et al., 2023), results show that chemical fertilizer, waste from P-related industries, domestic sewage, and excrement from livestock and poultry farming are the primary P sources.

The issues highlight the limitations in understanding the contribution of different sources and managing catchment P within the urbanization process. In this study, we combine the dataset of phosphate oxygen isotopes in global catchments, land use types, a Bayesian model and nonlinear curve fitting to quantitatively identify the shifts in P dynamic under the specific urbanization scenarios. Our research firstly provides a global estimate of the variation of catchment P loadings due to urban expansion and its implications for managing catchment P loads. Specifically, we demonstrate that (i) the coupling of the isotopic approach and a Bayesian model enables insights into the sources

controlling P input in global catchments, (ii) to better illustrate regional differences in P sources, it is necessary to combine the local $\delta^{18}\text{O}_{(\text{PO}_4)}$ values of endmembers and economic characteristics, and (iii) different stages of urbanization process drive phased dynamic characteristics of catchment P sources.

2. Methods

2.1. Data acquisition

The $\delta^{18}\text{O}_{(\text{PO}_4)}$ values from multiple end-members were used for the analysis of catchments P sources. Meanwhile, the land cover data were employed to calculate the proportion of urban area, reflecting the process of urbanization. $\delta^{18}\text{O}_{(\text{PO}_4)}$ values are obtained from published peer reviewed papers from 2002 to 2022 and our own work in the Yangtze River catchment (Tian, 2017; Wang, 2022). Peer reviewed papers contain the related research published in journals collected by searching Web of Science and CNKI, doctoral and master's graduation thesis by searching CNKI, ProQuest, National Science Library, Chinese Academy of Sciences and references cited by the related research. Search terms include “phosphate oxygen isotope or (delta O-18 or Oxygen Isotopes) of phosphate or Oxygen Isotopes in Phosphate) and (water or river or (Water or aquatic ecosystem) or freshwater or lake or sediment”, “(phospho* or P) cycl* and (phosphate oxygen isotope or (delta O-18 or Oxygen Isotopes) of phosphate or Oxygen Isotopes in Phosphate)” or “(((phospho* or P) cycl*) or (phosphate oxygen isotope or (delta O-18 or Oxygen Isotopes) of phosphate or Oxygen Isotopes in Phosphate)) and (water or river or (Water or aquatic ecosystem) or freshwater or lake or sediment)”. Finally, a total of 64 relevant references were retained. Our own work was conducted in 2019, we collected river water, soil, sediment, fertilizer, P rock, wastewater of the domestic and industrial discharge from the head water in the Tuotuo River to the estuary in Shanghai City in the Yangtze River. There are different ways of preparing Ag_3PO_4 for $\delta^{18}\text{O}_{(\text{PO}_4)}$ analyses, Amongst them, magnesium-induced coprecipitation (MAGIC) (McLaughlin et al., 2004), and ammonium phospho-molybdate precipitation and magnesium ammonium phosphate (APM-MAP) (Tamburini et al., 2010) are widely used and accepted. Detailed description of the two methods can be seen in SI Appendix 1 Part 1–3. $\delta^{18}\text{O}_{(\text{PO}_4)}$ values of literatures and our own work are mostly based on the two methods to extract and purify Ag_3PO_4 , except two publications, where they used different way to prepare Ag_3PO_4 , the reliability was proved equal to the MAGIC method, with a standard deviation of $\pm 0.3\%$ (Gruau et al., 2005; Liu et al., 2020). Therefore, the dataset of $\delta^{18}\text{O}_{(\text{PO}_4)}$ values collected from global catchments can be integrated and analysed for source apportionment of catchment P. The raw data and references cited can be seen in the SI Appendix 2.

Annual global land cover mapping at 300 m from 2002 to 2020 is derived from European Space Agency (ESA) Climate Change Initiative (CCI) (<https://cds.climate.copernicus.eu/cdsapp#!/dataset/satellite-land-cover?tab=overview>). This dataset provides global maps describing the land surface into 22 classes (Table S1), which have been defined using the United Nations Food and Agriculture Organization's (UN FAO) Land Cover Classification System (LCCS). The data format provided by the internet service is NetCDF4, we use the Model Builder in Arc GIS 10.7 to make a batch data format conversion from NetCDF4 to Geo TIFF. Similarly, we clip the land cover grid data based on the shape file of catchments boundary in batches by using Model Builder. Years of land use types are based on the sampling date provided by references. Then we reclarify the proportions of different land use types for the subsequent analysis and discussion (Table S1). Bottom maps of global catchment division derived from HydroBASINS (<https://www.hydrosheds.org/products/hydrobasins>), there are 12 levels of catchments classification. We choose the level 03 and level 04 to divide global catchments due to that the classification level of these is almost the same as the size of existing research areas. The size and number of catchment

divisions are shown in Fig. S1.

2.2. Data processing

To accurately illustrate the features of $\delta^{18}\text{O}_{(\text{PO}_4)}$ values in a specific catchment, we use the isotopic information of sources mainly based on relevant studies for this region. That is because the $\delta^{18}\text{O}_{(\text{PO}_4)}$ values of potential end members in the different catchments have large differences. The $\delta^{18}\text{O}_{(\text{PO}_4)}$ values of end members of the catchment itself can better quantify the proportions of potential P sources. The main focus of this study is the shifts in external P source of watersheds driven by urban expansion, therefore, four potential P sources (without considering internal P loadings) are used, including bedrock (bedrock weathering), fertilizer (agricultural fertilization), WWTP (urban domestic and industrial wastewater) and faeces (livestock and poultry breeding). We select the four P sources based on the existed studies. The four potential sources are the main drivers for catchment P loading. Detailed information on $\delta^{18}\text{O}_{(\text{PO}_4)}$ values selected and the relevant references cited can be seen in the SI Appendix 3–5. SI Appendix 3, 4 and 5 contains the $\delta^{18}\text{O}_{(\text{PO}_4)}$ values of the Asia, Europe and North America catchments, respectively. Locations and names of global catchments are shown in Fig. 1a.

In this study, we use the proportions of urban areas to reflect the level of urbanization process. Urban buildings usually remain for a long

term without returning to undeveloped land, urban expansion normally casts lasting effects on the connected environments (Gao and O'Neill, 2020). Due to the different social backgrounds, different catchments would have different population density, therefore, we did not use the population living in the urban area to illustrate the degree of urbanization. Urban areas can multi-dimensionally show a level of urbanization, agricultural labour changes and agricultural economic development (Bren d'Amour et al., 2017; Ma et al., 2019). Proportions of urban areas in catchments of existing research are shown in Table S2. Though study areas and years may differ from each other, we can take the proportions of urban areas in specific years and regions as a unified indicator to integrate the global $\delta^{18}\text{O}_{(\text{PO}_4)}$ values data for making a macro analysis of the P sources characteristics of the global catchments (Chen et al., 2020). Land covers of global catchments in 2020 were defined by the Model Builder in Arc GIS 10.7 and Python 3.7.

2.3. Statistical analysis

To meet the diverse computational and visualization needs of this study, we chose different software specialized in various areas for analysis. The computation of the Bayesian mixture model was performed using the *simmr* package in R, while the corresponding visualization was collaboratively accomplished by the *tidyverse* and *ggplot* packages. The nonlinear curve fitting of catchment P source proportions

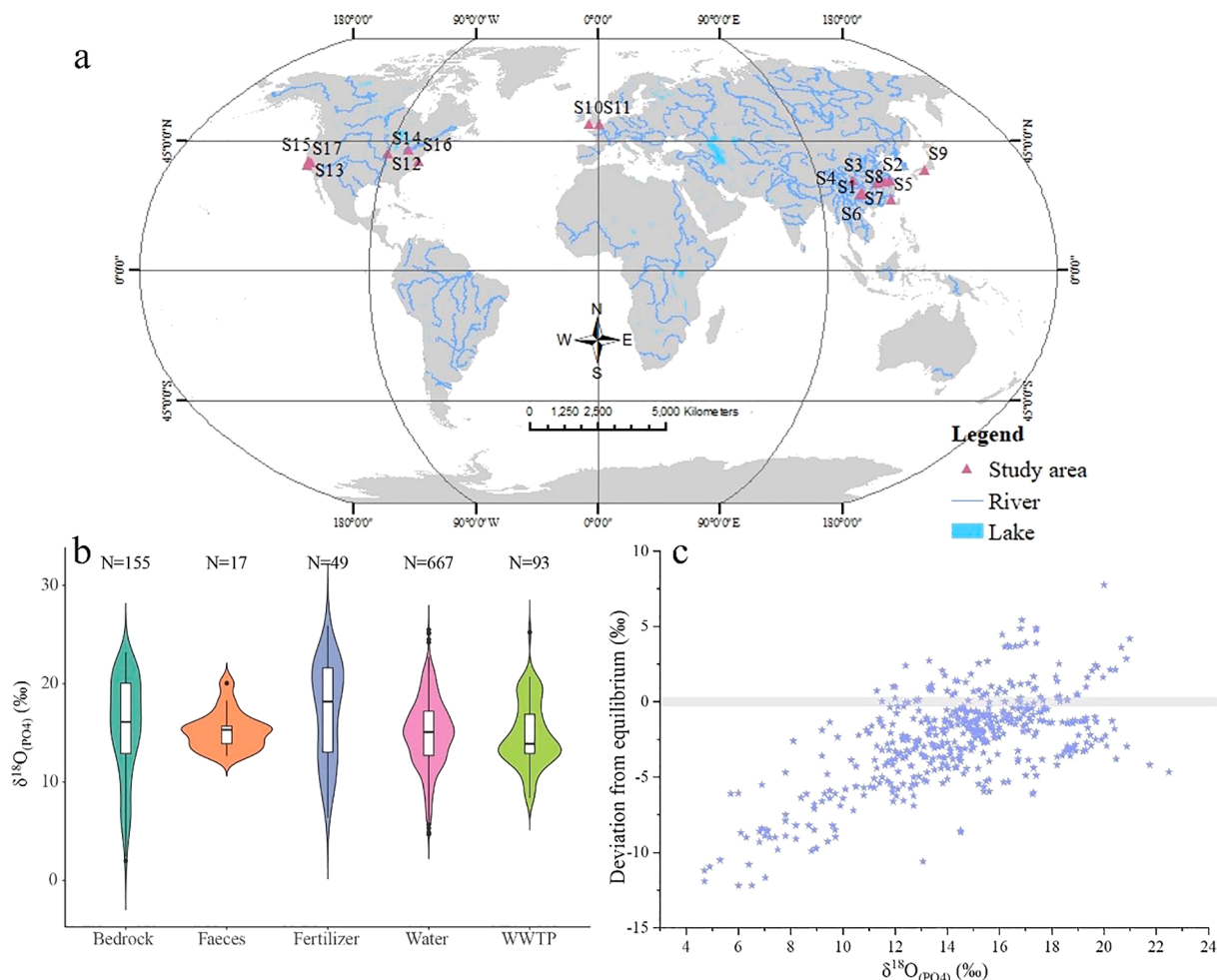


Fig. 1. Global distribution of study area and the dataset of $\delta^{18}\text{O}_{(\text{PO}_4)}$ values. a, The global distribution of catchments, S1: Hongfeng Lake, S2: Zhushanwan Bay, S3: Mianyuan River, S4: Yangtze River, S5: Jionglong River, S6: Tangxun Lake, S7: Aha Lake, S8: Yangshui River, S9: Yasu River, S10: River Taw catchment, S11: River Beult, S12: Lake Erie, S13: San Joaquin River, S14: Illinois River, S15: San Francisco Bay, S16: East Creek, S17: Monterey Bay. b, The datasets of $\delta^{18}\text{O}_{(\text{PO}_4)}$ values in five end members, we can directly see the distribution of the isotope values in different members. c, Deviation of the $\delta^{18}\text{O}_{(\text{PO}_4)}$ values measured from the expected equilibrium $\delta^{18}\text{O}_{(\text{PO}_4)}$ values, the grey shadow means that 95 % confidence interval for calculated equilibrium.

in response to urbanization was done using Origin Pro 2022. For map creation, we utilized the professional mapping software ArcGIS to achieve accurate depiction.

To quantitatively identify the P source in different catchments, we calculate the proportions of potential P sources in combination with the phosphate oxygen isotopes and a Bayesian model (Mingus et al., 2019; Parnell and Inger, 2021), the specific calculation process is illustrated in Eq. (1). Calculation and visualization of the results of the Bayesian model and proportions of main P sources in each catchment were performed in R 4.2.1. Stable Isotope Mixing Models in R with simmr allows full access to posterior densities of the Bayesian model (Parnell and Inger, 2021), so that we can create our calculation based on our needs. The formula is as follows:

$$\begin{aligned} \delta^{18}\text{O}_{(\text{PO}_4)} &= \delta^{18}\text{O}_{(\text{PO}_4\text{N}_1)} \times f_{\text{N}_1} + \delta^{18}\text{O}_{(\text{PO}_4\text{N}_2)} \times f_{\text{N}_2} + \delta^{18}\text{O}_{(\text{PO}_4\text{N}_3)} \times f_{\text{N}_3} \\ &\quad + \delta^{18}\text{O}_{(\text{PO}_4\text{N}_4)} \times f_{\text{N}_4} \\ f_{\text{N}_1} + f_{\text{N}_2} + f_{\text{N}_3} + f_{\text{N}_4} &= 1 \\ X_{ij} &= \sum_{k=1}^k P_k (S_{jk} + C_{jk}) + \varepsilon_{ij} \\ S_{jk} &\sim N(\mu_{jk}, \omega_{jk}^2) \\ C_{jk} &\sim N(\lambda_{jk}, \tau_{jk}^2) \\ \varepsilon_{ij} &\sim N(0, \sigma_j^2) \end{aligned} \quad (1)$$

Where $\delta^{18}\text{O}_{(\text{PO}_4)}$ is $\delta^{18}\text{O}_{(\text{PO}_4)}$ values of the water body, $\delta^{18}\text{O}_{(\text{PO}_4\text{N}_1)}$, $\delta^{18}\text{O}_{(\text{PO}_4\text{N}_2)}$, $\delta^{18}\text{O}_{(\text{PO}_4\text{N}_3)}$, $\delta^{18}\text{O}_{(\text{PO}_4\text{N}_4)}$ is the $\delta^{18}\text{O}_{(\text{PO}_4)}$ values of the end member. f_{N_1} , f_{N_2} , f_{N_3} , f_{N_4} is the contribution rate of the multiple P sources, X_{ij} is the isotope value j of the end member i ; P_k is the dietary proportion of source k , which estimated by the model; S_{jk} represents the isotopic value j of source value k , which follows the normal distribution with the mean μ_{jk} ; C_{jk} represents the fractionation coefficient of the isotope j on the source k , normally distributed with mean λ_{jk} and τ_{jk}^2 ; ε_{ij} is the residual error, describing additional inter-observation variance not described by the model, σ_j^2 is estimated by the model. As only the phosphate oxygen isotope is used, the value of j is 1 in this formula.

Sigmoidal fit by Origin Pro 2022 is used to illustrate the driving force of urbanization on the fertilizer P input. Function of Sigmoidal fit is the Logistic, the Iteration Algorithm uses Orthogonal Distance Regression (Pro). Impact of urban expansion on WWTP and faeces P loadings is to adopt a Nonlinear curve fitting, the category is the Piecewise. Function uses PWL2, the Iteration Algorithm of Orthogonal Distance Regression (Pro) is applied for this analysis. The expected equilibrium values ($\delta^{18}\text{O}_E$) of $\delta^{18}\text{O}_{(\text{PO}_4)}$ composition are estimated using the following modified equation (Chang and Blake, 2015):

$$\delta^{18}\text{O}_E = (\delta^{18}\text{O}_{(\text{H}_2\text{O})} + 1000) e^{\left(\frac{14.43 * 1000 - 26.54}{T} \right)} / 1000 - 1000 (r^2 = 0.99) \quad (2)$$

where $\delta^{18}\text{O}_{(\text{H}_2\text{O})}$ is the oxygen isotope composition (‰) of the ambient water, T is the temperature of water (°C), $\delta^{18}\text{O}_E$ is defined by temperature and $\delta^{18}\text{O}_{(\text{H}_2\text{O})}$.

The location and sampling map of the study area are drawn using Arc GIS 10.7. Significance test and Bayesian factor inference of Pearson correlation is conducted and visualized by the IBM SPSS Statistics 27. Violins are plotted in the R 4.2.1. Origin Pro 2022 is used to construct all the other data graphs.

3. Results and discussion

3.1. Current dataset of $\delta^{18}\text{O}_{(\text{PO}_4)}$ values in global catchments

In recent decades, research on catchments P source apportionment using $\delta^{18}\text{O}_{(\text{PO}_4)}$ values has primarily focused on the northern hemisphere (Fig. 1a). The northern hemisphere, characterized by higher population densities and complex river networks, presents distinct challenges compared to the southern hemisphere. The $\delta^{18}\text{O}_{(\text{PO}_4)}$ values of global freshwater and potential P sources exhibit a wide range and overlap amongst different end members (Fig. 1b). The $\delta^{18}\text{O}_{(\text{PO}_4)}$ values in global catchments range from 2.0 ‰ to 25.9 ‰, with an average value of 15.2 ± 3.9 ‰. Similarly, the $\delta^{18}\text{O}_{(\text{PO}_4)}$ values in global fresh water range from 4.7 ‰ to 25.0 ‰, the average value is 14.9 ± 3.6 ‰. $\delta^{18}\text{O}_{(\text{PO}_4)}$ values in global bedrock range from 2.0 ‰ to 23.2 ‰, with an average value of 15.6 ± 5.1 ‰. The wide range of $\delta^{18}\text{O}_{(\text{PO}_4)}$ values in the bedrock highlights significant geological differences on a global scale, with distinct $\delta^{18}\text{O}_{(\text{PO}_4)}$ signatures resulting from varying formation mechanisms (Smith et al., 2021). The $\delta^{18}\text{O}_{(\text{PO}_4)}$ values in global fertilizer range from 6.4 ‰ to 25.9 ‰, with an average value of 17.2 ± 5.0 ‰. For global WWTP, the $\delta^{18}\text{O}_{(\text{PO}_4)}$ values range from 8.4 ‰ to 25.2 ‰, with an average value of 14.8 ± 3.3 ‰. The wide range of isotope composition in WWTP indicates the strong human interference on P inputs (Goody et al., 2018). The $\delta^{18}\text{O}_{(\text{PO}_4)}$ values in global faeces range from 12.7 ‰ to 20.1 ‰, with an average value of 15.2 ± 2.0 ‰.

We compared the differences of the measured $\delta^{18}\text{O}_{(\text{PO}_4)}$ values with the theoretical equilibrium. Deviation between the calculated and measured $\delta^{18}\text{O}_{(\text{PO}_4)}$ values is as shown in Fig. 1c. The most measured $\delta^{18}\text{O}_{(\text{PO}_4)}$ values (about 95 %) are no longer found within the equilibrium range. Under these conditions, phosphate oxygen isotope technique can distinguish the potential P sources. In addition, we find that there is a significant ($p < 0.01$) positive correlation between the measured $\delta^{18}\text{O}_{(\text{PO}_4)}$ values and the deviation (Fig. S2). This is an interesting result which has not been realized previously although the reasons for this pattern need to be further investigated.

3.2. Contribution rate of multiple anthropogenic sources

Based on the analysis using the Bayesian model, probability density diagrams for each catchment are presented in Figs. S3–S5. These diagrams represent the likelihood of different outcomes and corresponding results of a random variable. Taking the example of Hongfeng Lake in 2014 (Fig. S3a), the probability density diagram shows that when the probability of wastewater treatment plants (WWTP) is approximately 65 %, it has the highest density value. Therefore, the contribution rate of WWTP to the P loadings in Hongfeng Lake is estimated to be around 65 %. A narrower credible interval indicates a lower level of uncertainty in the probability estimation (Parnell and Inger, 2021). On the other hand, in the case of Zhushan Bay in 2014 (Fig. S4c), the contribution of fertilizer appears to be less constrained compared to other sources, indicating a higher level of uncertainty in estimating its proportion. While it is possible that other potential P sources may not have been fully considered, the remaining three sources (bedrock, WWTP, and faeces) show more reliable proportion estimates. Therefore, the results obtained from the Bayesian model analysis still hold significant value for quantitative source analysis.

By using the results of the Bayesian model, the contributions of four potential P sources to freshwater P loadings in each catchment are displayed in Figs. S6–S8. These figures allow us to observe the temporal and spatial variations in the proportions of the four potential sources. The temporal variations can shed light on shifts in socio-economic characteristics and the implementation of water quality improvement measures. Taking Hongfeng Lake in Asia and Lake Erie in North America as examples, we can see changes in the contribution rates of WWTP over time. In Hongfeng Lake, the contribution rate of WWTP in 2022 (Fig. S6a) is significantly lower than that in 2014 (Fig. S6b), which can

be attributed to the implementation of various protection measures in the Yangtze River Catchment. These measures include (i) the implementation of an action plan for water pollution prevention (The State Council, 2015), (ii) establishment of the river chief system (The State Council, 2016), (iii) comprehensive regulation of black and odorous water bodies, and (iv) strict control of triphosphate chemical enterprises (Qu, 2021). These measures have contributed to the reduction of P input from WWTP. Consequently, the difference in proportions between WWTP and other sources has diminished over time. In Lake Erie, from 2005 (Fig. S8a) to 2014 (Fig. S8c), the proportion of WWTP P is much higher than that of the other sources. One reason is that internal P source is not considered, the internal P loadings estimates amount to 8–20% of the total external input of P to Lake Erie (Paytan et al., 2017). The other is that the proportion of urban area increased from 1.9 % to 2.2 % (Table S2), resulting in higher production of industrial and domestic sewage during this period. The increase in soluble P in Lake Erie is linked to changing anthropogenic activities (Depew et al., 2018), and it led to a resurgence of cyanobacterial blooms in 2011, likely driven by industrial and domestic sewage (Michalak et al., 2013).

On a global scale, the proportions of the four potential P sources exhibit significant regional differences (Fig. 2). These differences are closely related to the local socio-economic characteristics of each catchment. In the Aha Lake, Hongfeng Lake, and Yangshui River catchments, for instance, the rapid development of Triphosphate Chemical Enterprises (Ji, 2017; Liu, 2020; Xue, 2020) and expansion of urban areas (Table S2) have led to substantial P inputs from WWTP. Consequently, WWTP has become the largest source of P in these catchments. Similarly, in the River Taw Catchment and San Joaquin River catchments, the presence of densely distributed drain outlets and sewage treatment plants along the river (Granger et al., 2017; Young et al., 2009) has made WWTP the dominant P source (Fig. 2). In the Yangtze River, Zhushan Bay, and Monterey Bay catchments, intensive agricultural activities have made fertilizer the primary driver of high P loadings. These regions have experienced significant P inputs from

agricultural practices (Hu et al., 2020; McLaughlin et al., 2006a). The River Beult catchment, characterized by a considerable proportion (29.7 %) of grassland area (Table S2), shows a substantial contribution (40.6 %) of P from faeces (Fig. S7b), mainly attributed to livestock and poultry breeding, which contributes significantly to cultural eutrophication (Goody et al., 2016). Similarly, in the Jiulong River catchment, faeces contribute 42.5 % of the P loadings, even though the proportion of grassland area is only 0.8 % (Table S2). This is primarily due to the significant contribution of pig breeding, with more than 6.8 million pigs sold in 2015 (Fujian Provincial Bureau of Statistics, 2016).

3.3. Shifts in proportions of potential P sources with urban areas increase

Rapid urbanization can have severe consequences for the degradation of catchment ecosystems, primarily due to modifications in land-use types, pollution, and surface impermeabilization. (Fu et al., 2021; Yang et al., 2018) This urbanization process creates complex eutrophication scenarios (Archana et al., 2018). By employing nonlinear curve fitting, we observed a phased change trend in fertilizer P input with the increase of urban areas (Fig. 3a). During the initial stages of urbanization (proportion of urban areas <1.5 %), P input from agricultural fertilization remains low (7.8–14.3 %). Consequently, a higher percentage of P from WWTP (40.5 %–60.8 %) enters the catchments (Fig. 3b). Tong et al., found that the improvement of wastewater treatment facilities accompanying social and urban development would be the dominant reduction of urban domestic P loadings (Tong et al., 2020, 2017). Therefore, the low level of urbanization corresponds to a lower percentage of municipal wastewater being treated. Insufficient collection and treatment facilities, coupled with increasing wastewater production, contribute to the high proportions of P input from WWTP (Ma et al., 2020; Yu et al., 2019). As urbanization accelerates (1.5 % ≤ proportion of urban areas <3.5 %), the growing population’s demand for crop production (Elser and Bennett, 2011) leads to the increased mining of geological phosphate reserves for fertilizer production, catering to the

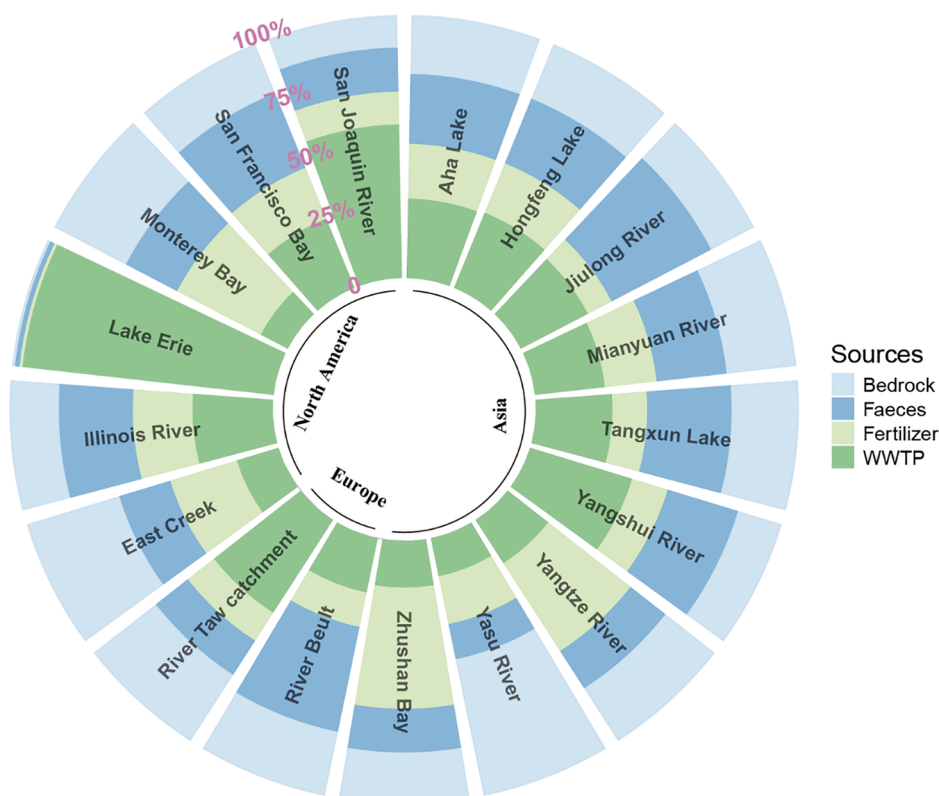


Fig. 2. Proportions of different drivers on catchments P loadings.

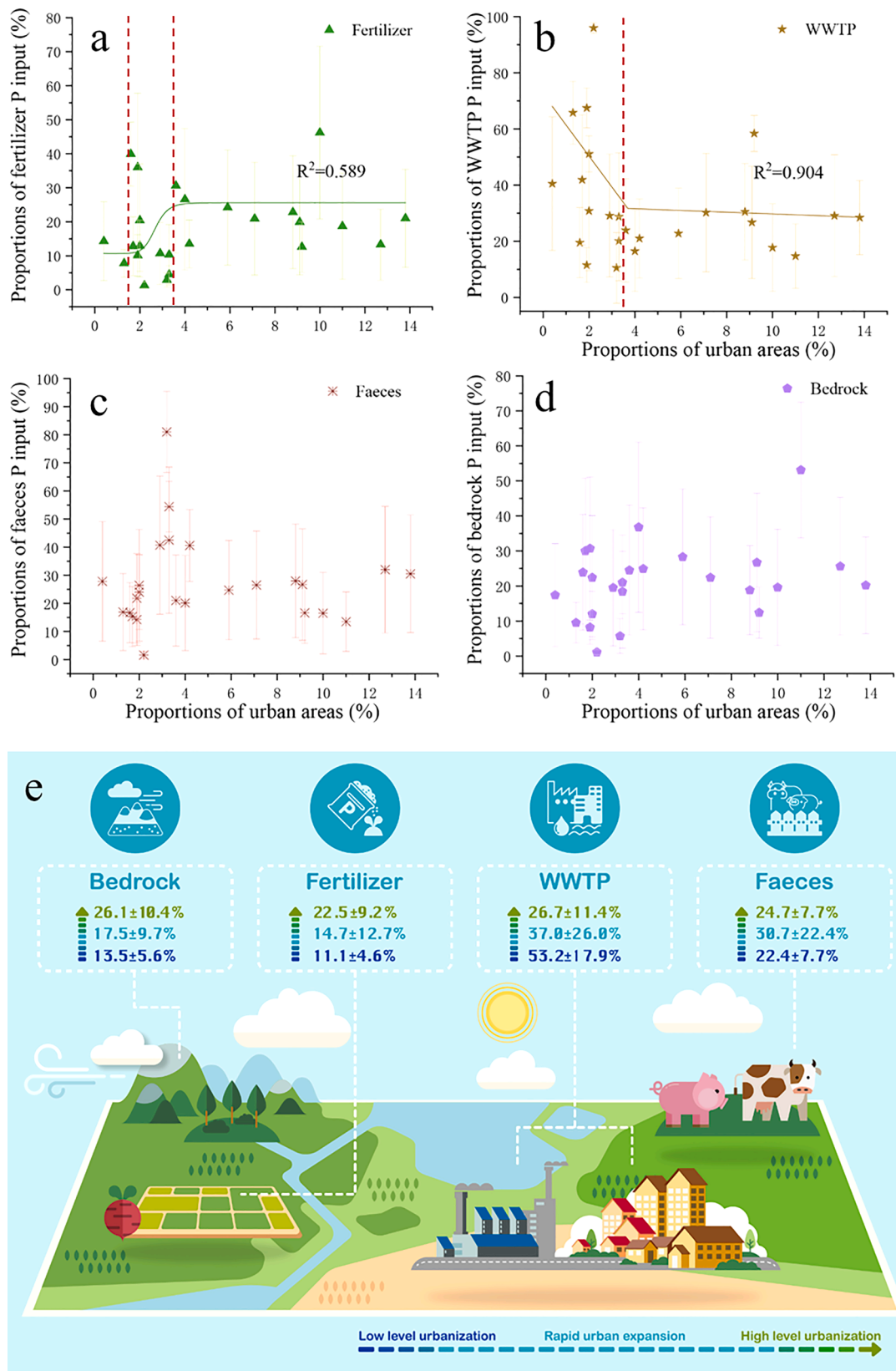


Fig. 3. Shifts in contributions of different sources with urban areas increased.

rising food demand (Tilman et al., 2001). Consequently, the proportions of fertilizer P input rise sharply (Fig. 3a), while the P input from WWTP into catchments noticeably decreases (Fig. 3b). This decrease is closely associated with the improvement in municipal wastewater treatment

(Tong et al., 2020). Wastewater treatment serves as a primary solution for reducing point-source water pollution, particularly in developing countries (Yu et al., 2019). In the third phase of the urbanization process (proportion of urban areas $\geq 3.5\%$), the proportions of agricultural

fertilization and WWTP P input tend to stabilize as urban areas increase (Fig. 3a, b). High levels of urbanization can lead to overconsumption of resources, resulting in the serious degradation of ecosystems (Li et al., 2022; Raudsepp-Hearne et al., 2010). In our study, high levels of urbanization did not cause a further increase in fertilizer P input. This does not imply a reduction in crop production, as higher population densities require increased food production (Nchanji and Nchanji, 2022; Zhang et al., 2016). The absence of further increases following urbanization may be due to crop production reaching its peak in areas with occupied croplands, and farms transforming into intensive industries (Liu et al., 2021). Additionally, the loss of croplands resulting from urban expansion (Bren d'Amour et al., 2017) and the shift from grain to economic crops (Liu et al., 2021; Wang et al., 2021) necessitate the transportation of more food crops from farther away. The reasons for the absence of further reductions in the proportions of WWTP P input can be attributed to the increasing sewage production as the population becomes more urbanized (Baojing et al., 2019) and the challenges associated with rural sewage treatment (Qu, 2021; Tong et al., 2020).

Concerning livestock and poultry breeding, the input of P from faeces does not exhibit an obvious increasing or decreasing trend during the urbanization process (Fig. 3c). However, high levels of urbanization can lead to shifts in dietary patterns (Pandey et al., 2020; Popkin, 1999), with increased consumption of animal products due to the higher income of the urban population (Seto and Ramankutty, 2016). Over the past 50 years, global P demand for food has tripled, from 2.8 Tg P to 8.8 Tg P (Chen and Graedel, 2016). The high consumption of meat products results in greater fertilizer application to farmland to increase crop yield (Tilman et al., 2001; Yuan et al., 2018). Problems arising from surplus livestock faeces P are becoming increasingly serious (Chen and Graedel, 2016; Zhao et al., 2022), with annual faeces P production equivalent to the application of P fertilizer (Bouwman et al., 2013). Due to intensive livestock and poultry management, a region occupying 13 % of the global planting area produces over 50 % of the global manure (Bai et al., 2014b; Mihelcic et al., 2011). Therefore, urbanization increases the production of P in faeces, but this increase in P loads is transferred to surrounding areas due to the centralized production and transportation of meat. Bedrock weathering primarily reflects the influence of natural factors on P loads in catchments, such as rainfall and bedrock properties. As a result, the urbanization process has little impact on Bedrock P input (Fig. 3d). We can consider P from this source as the natural background value.

In summary, the impact of urbanization on P loadings in catchments can be categorized into three stages based on the forces exerted by urban expansion on fertilizer and WWTP P input (Fig. 3e). This division aligns with the three-stage theory of urbanization development (Fang et al., 2008). During the early stage of low-level urbanization, although grain demand and sewage production may be relatively low, the excessive use of P fertilizer with low efficiency and inadequate sewage treatment facilities pose a serious threat to catchment ecosystems (Larsen et al., 2016; Tong et al., 2017). Domestic wastewater and agricultural activities serve as significant sources of P pollutants (Tong et al., 2017). Following this initial stage, catchment P loadings undergo a rapid transformation period of P sources as urbanization enters the mid-term acceleration stage. The rapid population growth and dietary improvements exert greater pressure on food supply, leading to increased application of fertilizer P to enhance crop yield. Consequently, excessive P enters aquatic systems (Tilman et al., 2001). Although environmental efforts focus on urban wastewater treatment and the provision of urban environmental infrastructure to reduce WWTP P input (Fig. 3b), the escalating discharges resulting from intensified agricultural activities pose a threat to these gains (Ma et al., 2020). During the high-level urbanization stage, urban expansion significantly impacts global catchment environments, with approximately half of urban growth occurring on existing croplands (Chen et al., 2020). This helps explain why the proportion of fertilizer P does not continuously increase with urban expansion (Fig. 3a). Cropland is consumed by urbanization,

leading to the emergence of urban agglomerations and metropolitan areas, and formerly productive agricultural land is lost to urbanization (Godfray et al., 2010). Farmers increasingly cultivate cash crops for higher economic income (Liu et al., 2021), and large-scale farming replaces small-scale farming due to rural land release and a decrease in the rural population (Wang et al., 2021). To meet the diverse and high-quality food demands of the urban population, a significant amount of grain and meat products are transported from other regions. Long-distance transportation transfers the P nutrients resulting from the food required for urbanization to remote areas, which bear the burden of catchment ecosystem degradation due to high P loadings from crop cultivation and livestock breeding.

3.4. P emission reduction strategies in global catchments

Based on the current global catchment urbanization area proportions (see Fig. S9), approximately 80 % to 85 % of catchments have an urban area proportion of ≤ 1.5 %. While the production of wastewater treatment plants (WWTPs) during the initial urbanization stage might be lower compared to the other two stages, the sewage treatment capacity remains inadequate. Since most global catchments are in the low urbanization stage, improving sewage treatment capacity and implementing comprehensive regulations for black and odorous water bodies are key measures to reduce anthropogenic P loads.

Around 8 % to 12 % of catchments have an urban area proportion between 1.5 % and 3.5 %. In this stage, as the global population becomes increasingly urbanized over time, substantial amounts of geological phosphate reserves are extracted for fertilizer production, supporting the Green Revolution (Elser and Bennett, 2011). Consequently, the proportion of fertilizer P input experiences a rapid increase, necessitating heightened attention to agricultural non-point source pollution. Although the amount of P input from WWTPs gradually decreases, its proportion remains relatively significant. Therefore, it is crucial to focus on improving the treatment rate of industrial tailwater and domestic sewage.

Approximately 6 % to 8 % of catchments have an urban area proportion exceeding 3.5 %. During the high-level urbanization stage, the contribution rates of P from WWTPs and fertilizers tend to stabilize. Agricultural practices tend to become large-scale, and substantial amounts of food are transported to urban agglomerations to feed the dense population. Implementing cost-effective rural sewage treatment becomes crucial for further reducing WWTP P input. Reducing the application of fertilizer P and enhancing its efficiency would also be beneficial in decreasing fertilizer P input. Furthermore, as the urban population increases, proper utilization of faeces and prevention of unsystematic accumulation become imperative, particularly with the rise in meat product consumption.

4. Conclusion

Phosphate oxygen isotope is an effective tracer for identifying P sources. Urbanization drives changes in the dynamic characteristics of catchment P loadings. Different stages of urbanization correspond to distinct anthropogenic P source characteristics. In the early stages of urbanization, the P input from WWTP has the greatest impact on catchment P loadings due to insufficient sewage treatment capacity. During the rapid urbanization period, environmental efforts primarily focus on wastewater treatment, resulting in a noticeable reduction in WWTP P input. However, the increased use of fertilizers in croplands to meet the demands of a growing population offsets the benefits of reduced sewage P. In the final stage, as urban construction replaces agricultural land, intensified and mechanized farming practices, as well as long-distance transportation of food, contribute to stable WWTP and fertilizer P input levels. Further urbanization places excessive P loading stress on remote areas due to increasing food demand and improvements in the urban population's dietary structure. Based on different

urbanization characteristics, specific catchment P management strategies can be proposed to achieve the goal of improving water quality in catchments.

Synopsis

Minimal research exists on variations of catchment P sources driven by urbanization. This study firstly provides a global estimate of catchment P loadings shifts with urban expansion and its implications for managing catchment P loads

CRedit authorship contribution statement

Ziteng Wang: Conceptualization, Data curation, Formal analysis, Investigation, Methodology, Project administration, Resources, Software, Supervision, Validation, Visualization, Writing – original draft, Writing – review & editing. **Fuhong Sun:** Data curation, Formal analysis, Funding acquisition, Resources, Software, Supervision, Writing – review & editing. **Qingjun Guo:** Data curation, Methodology, Writing – review & editing. **Daren C. Goody:** Writing – review & editing. **Fengchang Wu:** Funding acquisition, Investigation, Methodology, Software, Supervision, Writing – review & editing.

Declaration of Competing Interest

All authors declare they have no competing interests and there are no other relationships or activities that could appear to have influenced the submitted work.

Data availability

Data will be made available on request.

Acknowledgements

This work was financially supported by the National Key Research and Development Program (No. 2021YFC3201001), National Natural Science Foundation of China (No. 42230713), and Joint Research Project for the Yangtze River Conservation (Phase II), China (NO. 2022-LHYJ-02-0101). We appreciate the editors and anonymous referees for their constructive comments.

Supplementary materials

Supplementary material associated with this article can be found, in the online version, at [doi:10.1016/j.watres.2023.121026](https://doi.org/10.1016/j.watres.2023.121026).

References

- Archana, A., Thibodeau, B., Geeraert, N., Xu, M.N., Kao, S.J., Baker, D.M., 2018. Nitrogen sources and cycling revealed by dual isotopes of nitrate in a complex urbanized environment. *Water Res.* 142, 459–470.
- Bai, X., Shi, P., Liu, Y., 2014a. Realizing China's urban dream. *Nature* 509, 158–160.
- Bai, Z.H., Ma, L., Qin, W., Chen, Q., Oenema, O., Zhang, F.S., 2014b. Changes in Pig Production in China and Their Effects on Nitrogen and Phosphorus Use and Losses. *Environ. Sci. Technol.* 48 (21), 12742–12749.
- Baojing, G., Xiaoling, Z., Xuemei, B., Bojie, F., Deli, C., 2019. Four steps to food security for swelling cities. *Nature* 566, 31–33.
- Bi, P., Huang, G., Liu, C., Li, L., 2022. Geochemical factors controlling natural background levels of phosphate in various groundwater units in a large-scale urbanized area. *J. Hydrol. (Amst)* 608 (2022), 127594.
- Bouwman, L., Goldewijk, K.K., Van Der Hoek, K.W., Beusen, A.H.W., Van Vuuren, D.P., Willems, J., Rufino, M.C., Stehfest, E., 2013. Exploring global changes in nitrogen and phosphorus cycles in agriculture induced by livestock production over the 1900–2050 period. *Proc. Natl. Acad. Sci. U.S.A.* 110 (52), 20882–20887.
- Bren d'Amour, C., Reitsma, F., Baiocchi, G., Barthel, S., Guneralp, B., Erb, K.H., Haberl, H., Creutzig, F., Seto, K.C., 2017. Future urban land expansion and implications for global croplands. *Proc. Natl. Acad. Sci. USA.* 114 (34), 8939–8944.
- Chang, S.J., Blake, R.E., 2015. Precise calibration of equilibrium oxygen isotope fractionations between dissolved phosphate and water from 3 to 37°C. *Geochim. Cosmochim. Acta* 150, 314–329.
- Chen, G., Li, X., Liu, X., Chen, Y., Liang, X., Leng, J., Xu, X., Liao, W., Qiu, Y., Wu, Q., Huang, K., 2020. Global projections of future urban land expansion under shared socioeconomic pathways. *Nat. Commun.* 11 (1), 537.
- Chen, M., Graedel, T.E., 2016. A half-century of global phosphorus flows, stocks, production, consumption, recycling, and environmental impacts. *Glob. Environ. Chang.* 36 (2016), 139–152.
- Cleveland, C.C., Liptzin, D., 2007. C:N:P stoichiometry in soil: is there a "Redfield ratio" for the microbial biomass? *Biogeochemistry* 85 (3), 235–252.
- Colman, A.S. (2002) The oxygen isotope composition of dissolved inorganic phosphate and the marine phosphorus cycle.
- Davies, C.L., Surridge, B.W.J., Goody, D.C., 2014. Phosphate oxygen isotopes within aquatic ecosystems: global data synthesis and future research priorities. *Sci. Total Environ.* 496, 563–575.
- Depew, D.C., Koehler, G., Hiriart-Baer, V., 2018. Phosphorus Dynamics and Availability in the Nearshore of Eastern Lake Erie: insights From Oxygen Isotope Ratios of Phosphate. *Front. Mar. Sci.* 5.
- Elser, J., Bennett, E., 2011. A broken biogeochemical cycle. *Nature* 478 (7367), 29–31.
- Fang, C., Liu, X., Lin, X., 2008. Stages correction and regularity analysis of urbanization of urbanization course of China. *Arid Land Geogr.* 31 (4), 513–523.
- Fu, H., Gauzere, P., Garcia Molinos, J., Zhang, P., Zhang, H., Zhang, M., Niu, Y., Yu, H., Brown, L.E., Xu, J., 2021. Mitigation of urbanization effects on aquatic ecosystems by synchronous ecological restoration. *Water Res.* 204, 117587.
- Fujian Provincial Bureau of Statistics, 2016. *Fujian Statistical Yearbook*.
- Gao, J., O'Neill, B.C., 2020. Mapping global urban land for the 21st century with data-driven simulations and shared socioeconomic pathways. *Nat. Commun.* 11 (1), 2302.
- Godfray, H.C.J., Beddington, J.R., Crute, I.R., Haddad, L., Lawrence, D., Mui, J.F., Pretty, J., Robinson, S., Thomas, S.M., Toulmin, C., 2010. Food security: the challenge of feeding 9 billion people. *Science* 327, 812–818.
- Goody, D.C., Bowes, M.J., Lapworth, D.J., Lamb, A.L., Williams, P.J., Newton, R.J., Davies, C.L., Surridge, B.W.J., 2018. Evaluating the stable isotopic composition of phosphate oxygen as a tracer of phosphorus from waste water treatment works. *Appl. Geochem.* 95, 139–146.
- Goody, D.C., Lapworth, D.J., Ascott, M.J., Bennett, S.A., Heaton, T.H., Surridge, B.W., 2015. Isotopic fingerprint for phosphorus in drinking water supplies. *Environ. Sci. Technol.* 49 (15), 9020–9028.
- Goody, D.C., Lapworth, D.J., Bennett, S.A., Heaton, T.H.E., Williams, P.J., Surridge, B.W.J., 2016. A multi-stable isotope framework to understand eutrophication in aquatic ecosystems. *Water Res.* 88, 623–633.
- Granger, S.J., Heaton, T.H.E., Pfahler, V., Blackwell, M.S.A., Yuan, H., Collins, A.L., 2017. The oxygen isotopic composition of phosphate in river water and its potential sources in the Upper River Taw catchment, UK. *Sci. Total Environ.* 574, 680–690.
- Gruau, G., Legeas, M., Riou, C., Gallacrier, E., Martineau, F., Henin, O., 2005. The oxygen isotope composition of dissolved anthropogenic phosphates: a new tool for eutrophication research? *Water Res.* 39 (1), 232–238.
- Ho, J.C., Michalak, A.M., Pahlevan, N., 2019. Widespread global increase in intense lake phytoplankton blooms since the 1980s. *Nature* 574 (7780), 667. ++.
- Hu, M., Liu, Y., Zhang, Y., Shen, H., Yao, M., Dahlgren, R.A., Chen, D., 2020. Long-term (1980–2015) changes in net anthropogenic phosphorus inputs and riverine phosphorus export in the Yangtze River basin. *Water Res.* 177, 115779.
- Huang, G., Liu, C., Zhang, Y., Chen, Z., 2020. Groundwater is important for the geochemical cycling of phosphorus in rapidly urbanized areas: a case study in the Pearl River Delta. *Environ. Pollut.* 260, 114079.
- Huang, G., Pei, L., Li, L., Liu, C., 2022. Natural background levels in groundwater in the Pearl River Delta after the rapid expansion of urbanization: a new pre-selection method. *Sci. Total Environ.* 813, 151890.
- Huang, G., Song, J., Han, D., Liu, R., Liu, C., Hou, Q., 2023. Assessing natural background levels of geogenic contaminants in groundwater of an urbanized delta through removal of groundwaters impacted by anthropogenic inputs: new insights into driving factors. *Sci. Total Environ.* 857 (Pt 2), 159527.
- Ide, J.I., Ishida, T., Cid-Andres, A.P., Osaka, K.I., Iwata, T., Hayashi, T., Akashi, M., Tayasu, I., Paytan, A., Okuda, N., 2020. Factors characterizing phosphate oxygen isotope ratios in river water: an inter-watershed comparison approach. *Limnology* 21 (3), 365–377.
- Ishida, T., Uehara, Y., Iwata, T., Cid-Andres, A.P., Asano, S., Ikeya, T., Osaka, K., Ide, J., Privaldos, O.L.A., Jesus, I.B.B., Peralta, E.M., Trino, E.M.C., Ko, C.Y., Paytan, A., Tayasu, I., Okuda, N., 2019. Identification of phosphorus sources in a watershed using a phosphate oxygen isoscape approach. *Environ. Sci. Technol.* 53 (9), 4707–4716.
- Ji, Y., 2017. Using Oxygen Isotope Composition of Phosphate to Trace Internal Phosphorus Release from Sediments of Deep-Water Lakes in Mountain area: Taking Hongfeng Lake As an Example. Institute of Geochemistry, Chines Academy of Sciences.
- Larsen, T.A., Hoffmann, S., Lüthi, C., Truffer, B., Maurer, M., 2016. Emerging solutions to the water challenges of an urbanizing world. *Science* 352 (6288), 928–933.
- Li, W., An, M., Wu, H., An, H., Huang, J., Khanal, R., 2022. The local coupling and telecoupling of urbanization and ecological environment quality based on multisource remote sensing data. *J. Environ. Manag.* 327, 116921.
- Liang, S., Yu, Y., Kharrazi, A., Fath, B.D., Feng, C., Daigger, G.T., Chen, S., Ma, T., Zhu, B., Mi, Z., Yang, Z., 2020. Network resilience of phosphorus cycling in China has shifted by natural flows, fertilizer use and dietary transitions between 1600 and 2012. *Nat. Food* 1 (6), 365–375.
- Liang, Y. (2005) Oxygen isotope studies of biogeochemical cycling of phosphorus.

- Liu, D., Li, X., Zhang, Y., Qiao, Q., Bai, L., 2023. Using a multi-isotope approach and isotope mixing models to trace and quantify phosphorus sources in the Tuojiang River, Southwest China. *Environ. Sci. Technol.* 57 (19), 7328–7335.
- Liu, X., Xu, Y., Engel, B.A., Sun, S., Zhao, X., Wu, P., Wang, Y., 2021. The impact of urbanization and aging on food security in developing countries: the view from Northwest China. *J. Clean. Prod.* 292 (2021), 126067.
- Liu, Y., 2020. Construction and Preliminary Application of Pretreatment Method System of Phosphate Oxygen Isotope Separation and Purification For Freshwater Lake Environmental Media. Institute of Geochemistry, Chinese Academy of Sciences.
- Liu, Y., Wang, J., Chen, J., Jin, Z., Ding, S., Yang, X., 2020. Method for phosphate oxygen isotopes analysis in water based on in situ enrichment, elution, and purification. *J. Environ. Manage.*, 111618. -111618.
- Ma, L., Long, H., Zhang, Y., Tu, S., Ge, D., Tu, X., 2019. Agricultural labor changes and agricultural economic development in China and their implications for rural vitalization. *J. Geog. Sci.* 29 (2), 163–179.
- Ma, T., Zhao, N., Ni, Y., Yi, J., Wilson, J.P., He, L., Du, Y., Pei, T., Zhou, C., Song, C., Cheng, W., 2020. China's improving inland surface water quality since 2003. *Sci. Adv.* 6, eaau3798.
- Mao, Y., Zhang, H., Cheng, Y., Zhao, J., Huang, Z., 2023. The characteristics of nitrogen and phosphorus output in China's highly urbanized Pearl River Delta region. *J. Environ. Manage.* 325 (Pt B), 116543.
- McLaughlin, K., Cade-Menun, B.J., Paytan, A., 2006a. The oxygen isotopic composition of phosphate in Elkhorn Slough, California: a tracer for phosphate sources. *Estuar. Coast. Shelf Sci.* 70 (3), 499–506.
- McLaughlin, K., Kendall, C., Silva, S.R., Young, M., Paytan, A., 2006b. Phosphate oxygen isotope ratios as a tracer for sources and cycling of phosphate in North San Francisco Bay, California. *J. Geophys. Res.-Biogeosci.* 111 (G3), 1–12.
- McLaughlin, K., Silva, S., Kendall, C., Stuart-Williams, H., Paytan, A., 2004. A precise method for the analysis of delta O-18 of dissolved inorganic phosphate in seawater. *Limnol. Oceanogr. Methods* 2, 202–212.
- Michalak, A.M., Anderson, E.J., Beletsky, D., Boland, S., Bosch, N.S., Bridgeman, T.B., Chaffin, J.D., Cho, K., Confesor, R., Daloglu, I., Depinto, J.V., Evans, M.A., Fahnenstiel, G.L., He, L., Ho, J.C., Jenkins, L., Johengen, T.H., Kuo, K.C., Laporte, E., Liu, X., McWilliams, M.R., Moore, M.R., Posselt, D.J., Richards, R.P., Scavia, D., Steiner, A.L., Verhamme, E., Wright, D.M., Zagorski, M.A., 2013. Record-setting algal bloom in Lake Erie caused by agricultural and meteorological trends consistent with expected future conditions. *Proc. Natl. Acad. Sci. USA.* 110 (16), 6448–6452.
- Mihelcic, J.R., Fry, L.M., Shaw, R., 2011. Global potential of phosphorus recovery from human urine and feces. *Chemosphere* 84 (6), 832–839.
- Mingus, K.A., Liang, X., Massoudieh, A., Jaisi, D.P., 2019. Stable isotopes and Bayesian modeling methods of tracking sources and differentiating bioavailable and recalcitrant phosphorus pools in suspended particulate matter. *Environ. Sci. Technol.* 53 (1), 69–76.
- Nchanji, E.B., Nchanji, Y.K., 2022. Urban farmers coping strategies in the wake of urbanization and changing market in Tamale, Northern Ghana. *Land Use Policy* 121, 106312.
- Pandey, B., Reba, M., Joshi, P.K., Seto, K.C., 2020. Urbanization and food consumption in India. *Sci. Rep.* 10 (1), 17241.
- Parnell, A. and Inger, R. 2021 **Stable Isotope Mixing Models in R with Simmr**.
- Paytan, A., Roberts, K., Watson, S., Peek, S., Chuang, P.C., Defforey, D., Kendall, C., 2017. Internal loading of phosphate in Lake Erie Central Basin. *Sci. Total Environ.* 579, 1356–1365.
- Popkin, B.M., 1999. Urbanization, lifestyle changes and the nutrition transition. *World Dev.* 27 (11), 1905–1916.
- Powers, S.M., Bruilsema, T.W., Burt, T.P., Chan, N.I., Elser, J.J., Haygarth, P.M., Howden, N.J.K., Jarvie, H.P., Lyu, Y., Peterson, H.M., Sharpley, A.N., Shen, J., Worrall, F., Zhang, F., 2016. Long-term accumulation and transport of anthropogenic phosphorus in three river basins. *Nat. Geosci.* 9 (5), 353. +-.
- Qu, J., 2021. Yangtze River Protection: How to Reduce Emissions in Depth? Yangtze Institute for Conservation and Development.
- Raudsepp-Hearne, C., Peterson, G.D., Bennett, E.M., 2010. Ecosystem service bundles for analyzing tradeoffs in diverse landscapes. *Proc. Natl. Acad. Sci. USA.* 107 (11), 5242–5247.
- Ryan, R.J., Packman, A.I., Kilham, S.S., 2007. Relating phosphorus uptake to changes in transient storage and streambed sediment characteristics in headwater tributaries of Valley Creek, an urbanizing watershed. *J. Hydrol. (Amst)* 336 (3–4), 444–457.
- Seto, K.C., Ramankutty, N., 2016. Hidden linkages between urbanization and food systems. *Science* 352, 943–945.
- Smith, A.C., Pfahler, V., Tamburini, F., Blackwell, M.S.A., Granger, S.J., 2021. A review of phosphate oxygen isotope values in global bedrocks: characterising a critical endmember to the soil phosphorus system. *J. Plant Nutr. Soil Sci.* 184 (1), 25–34.
- Steffen, W., Richardson, K., Rockstrom, J., Cornell, S.E., Fetzer, I., Bennett, E.M., Biggs, R., Carpenter, S.R., de Vries, W., de Wit, C.A., Folke, C., Gerten, D., Heinke, J., Mace, G.M., Persson, L.M., Ramanathan, V., Reyers, B., Sorlin, S., 2015. Sustainability. Planetary boundaries: guiding human development on a changing planet. *Science* 347 (6223), 1259855.
- Tamburini, F., Bernasconi, S.M., Angert, A., Weiner, T., Frossard, E., 2010. A method for the analysis of the delta O-18 of inorganic phosphate extracted from soils with HCl. *Eur. J. Soil Sci.* 61 (6), 1025–1032.
- Tcaci, M., Barbecot, F., Helie, J.F., Surridge, B.W.J., Goody, D.C., 2019. A new technique to determine the phosphate oxygen isotope composition of freshwater samples at low ambient phosphate concentration. *Environ. Sci. Technol.* 53 (17), 10288–10294.
- The State Council, 2015. Action Plan for Water Pollution Prevention. The State Council The People's Republic of China, Beijing.
- The State Council, 2016. Opinions On the Overall Implementation of the River Chief System. The State Council The People's Republic of China, Beijing.
- Tian, L. 2017 **The research of analysis method of oxygen isotope and its application of phosphate in agricultural soils**.
- Tilman, D., Fargione, J., Wolff, B., D'Antonio, C., Dobson, A., Howarth, R., Schindler, D., Schlesinger, W.H., Simberloff, D., Swackhamer, D., 2001. Forecasting agriculturally driven global environmental change. *Science* 292 (5515), 281–284.
- Tong, Y., Wang, M., Penuelas, J., Liu, X., Paerl, H.W., Elser, J.J., Sardans, J., Couture, R. M., Larssen, T., Hu, H., Dong, X., He, W., Zhang, W., Wang, X., Zhang, Y., Liu, Y., Zeng, S., Kong, X., Janssen, A.B.G., Lin, Y., 2020. Improvement in municipal wastewater treatment alters lake nitrogen to phosphorus ratios in populated regions. *Proc. Natl. Acad. Sci. USA.* 117 (21), 11566–11572.
- Tong, Y., Zhang, W., Wang, X., Couture, R.M., Larssen, T., Zhao, Y., Li, J., Liang, H., Liu, X., Bu, X., He, W., Zhang, Q., Lin, Y., 2017. Decline in Chinese lake phosphorus concentration accompanied by shift in sources since 2006. *Nat. Geosci.* 10 (7), 507–511.
- Wang, S., Bai, X., Zhang, X., Reis, S., Chen, D., Xu, J., Gu, B., 2021. Urbanization can benefit agricultural production with large-scale farming in China. *Nat. Food* 2 (3), 183–191.
- Wang, Z., 2022. Spatiotemporal Dynamics and Quantitative Source Analysis of Phosphorus in the Yangtze River Main Stream. Institute of Geographic Sciences and Natural Resources Research, Chinese Academy of Sciences.
- Wang, Z., Tian, L., Zhao, C., Du, C., Zhang, J., Sun, F., Tekleab, T.Z., Wei, R., Fu, P., Goody, D.C., Guo, Q., 2023. Source partitioning using phosphate oxygen isotopes and multiple models in a large catchment. *Water Res.* 244, 120382.
- Wells, N.S., Goody, D.C., Reshid, M.Y., Williams, P.J., Smith, A.C., Eyre, B.D., 2022. Delta(18)O as a tracer of PO4(3-) losses from agricultural landscapes. *J. Environ. Manage.* 317, 115299.
- Xue, K., 2020. The Impact of Phosphate Mining Activities on Surface Water Environment and Its Control Strategies – Insights from Phosphate Oxygen Isotope Tracing Technology. Institute of Geochemistry, Chinese Academy of Sciences.
- Yang, K., Pan, M., Luo, Y., Chen, K., Zhao, Y., Zhou, X., 2018. A time-series analysis of urbanization-induced impervious surface area extent in the Dianchi Lake watershed from 1988 to 2017. *Int. J. Remote Sens.* 40 (2), 573–592.
- Young, M.B., McLaughlin, K., Kendall, C., Stringfellow, W., Rollog, M., Elsbury, K., Donald, E., Paytan, A., 2009. Characterizing the oxygen isotopic composition of phosphate sources to aquatic ecosystems. *Environ. Sci. Technol.* 43 (14), 5190–5196.
- Yu, C., Huang, X., Chen, H., Godfray, H.C.J., Wright, J.S., Hall, J.W., Gong, P., Ni, S., Qiao, S., Huang, G., Xiao, Y., Zhang, J., Feng, Z., Ju, X., Ciais, P., Stenseth, N.C., Hesse, D.O., Sun, Z., Yu, L., Cai, W., Fu, H., Huang, X., Zhang, C., Liu, H., Taylor, J., 2019. Managing nitrogen to restore water quality in China. *Nature* 567 (7749), 516–520.
- Yuan, H., Wang, H., Dong, A., Zhou, Y., Huang, R., Yin, H., Zhang, L., Liu, E., Li, Q., Jia, B., Cai, Y., 2022. Tracing the sources of phosphorus in lake at watershed scale using phosphate oxygen isotope (delta(18)OP). *Chemosphere* 305, 135382.
- Yuan, Z., Jiang, S., Sheng, H., Liu, X., Hua, H., Liu, X., Zhang, Y., 2018. Human perturbation of the global phosphorus cycle: changes and consequences. *Environ. Sci. Technol.* 52 (5), 2438–2450.
- Zhang, F., Huang, G., Hou, Q., Liu, C., Zhang, Y., Zhang, Q., 2019. Groundwater quality in the Pearl River Delta after the rapid expansion of industrialization and urbanization: distributions, main impact indicators, and driving forces. *J. Hydrol.* 577 (2022), 124004.
- Zhang, M., Huang, G., Liu, C., Zhang, Y., Chen, Z., Wang, J., 2020. Distributions and origins of nitrate, nitrite, and ammonium in various aquifers in an urbanized coastal area, south China. *J. Hydrol.* 582 (2020), 124528.
- Zhang, W., Li, X., Swaney, D.P., Du, X., 2016. Does food demand and rapid urbanization growth accelerate regional nitrogen inputs? *J. Clean. Prod.* 112, 1401–1409.
- Zhao, S., Chen, Y., Gu, X., Zheng, M., Fan, Z., Luo, D., Luo, K., Liu, B., 2022. Spatiotemporal variation characteristics of livestock manure nutrient in the soil environment of the Yangtze River Delta from 1980 to 2018. *Sci. Rep.* 12 (1), 7353.